American Mineralogist, Volume 61, pages 1259–1266, 1976

Synthesis and metastable phase transformations of Na–, Na,K– and K–ferrierites

WILLIAM E. CORMIER[1] AND LEONARD B. SAND

Department of Chemical Engineering
Worcester Polytechnic Institute
Worcester, Massachusetts 01609

Abstract

Conditions are reported for the crystallization of Na–, Na,K– and K–ferrierites. A complete series exists between the end members, Na–ferrierite and K–ferrierite. Isothermal phase-transformation diagrams are given to show the kinetics of crystallization and the transformations of metastable ferrierites as a function of Na/K and CO_3/HCO_3 ratios in the starting compositions. The metastable ferrierites transform either to an intermediate mordenite phase or directly to quartz and feldspar. This mechanism is proposed as a possible explanation for ferrierite and mordenite of similar compositions occurring together in natural deposits. Ferrierite preferentially incorporates potassium into its structure over sodium. The feldspar formed by the transformation of ferrierite exhibits the same preference.

Well-crystallized ferrierite was obtained in the temperature range of 290–310°C with reaction times of 2–96 hours, using co-precipitated alumina–silica gels and Na– and K–bicarbonates and carbonates as reactant materials.

Introduction

The purpose of this study was to delineate the synthesis conditions for the formation of Na,K–ferrierites. The significant feature of the crystal structure of ferrierite is the existence of ten-membered rings parallel to the *c* axis. Nearly spherical cavities are connected to the ten-membered ring channels by eight-membered ring "windows." These windows define a secondary eight-membered ring channel system parallel to the *b* axis (Vaughan, 1966; Kerr, 1966).

Ferrierite with the unit-cell composition $Na_{1.26}K_{0.24}Mg_{2.0}Si_{30.5}Al_{5.5}O_{72} \cdot 18H_2O$ occurs at Kamloops Lake, British Columbia, with quartz and calcite (Vaughan, 1966; Graham, 1918); $Na_{1.29}K_{2.98}Mg_{0.31}Ca_{0.53}Si_{30.05}Al_{5.95}O_{72} \cdot 12H_2O$ at Pershing County, Nevada, with mordenite and tridymite (Sand and Regis, 1966); $Na_{0.25}K_{0.51}Ca_{0.99}Mg_{2.98}Fe^{3+}_{1.20}Al_{7.25}Si_{27.5}O_{72} \cdot 12H_2O$ at Vicenza, Italy, with calcite (Alietti *et al.*, 1967); and $Na_{1.87}K_{1.47}Ca_{0.05}Mg_{0.62}Si_{31.39}Al_{4.59}O_{72} \cdot 18.2H_2O$ at Ayoura, California, with clinoptilolite, quartz, and calcite (Wise *et al.*, 1969).

Senderov (1963), without specifying exact starting (batch) compositions, reported the synthesis of Na–ferrierite. Crystallization was achieved in the temperature range of 150–350°C, using silica gel, sodium aluminate, and sodium hydroxide as reactant materials in mixtures, giving a silica to alumina ratio of 10 and slight excess of Na_2O.

Barrer and Marshall (1965) reported the synthesis of Sr–ferrierite in the temperature range of 340–380°C from aqueous gels of composition $SrO : Al_2O_3 : 7\text{–}9SiO_2$. Hawkins (1967) synthesized Sr– and Ca–ferrierite at temperatures of 350–370°C from co-precipitated gels using nitrates of calcium, strontium, aluminum and Ludox colloidal silica sol. Sand (1968) reported Na–ferrierite as a coexisting phase with mordenite but no conditions for its synthesis were given.

Experimental

The chemical system $Na_2O \cdot K_2O \cdot Al_2O_3 \cdot H_2O \cdot CO_2 \cdot HCO_2$ was chosen for investigation because of the association of calcite with natural ferrierite (Graham, 1918; Alietti *et al.*, 1967; Wise *et al.*, 1969), the occurrence of Na,K–ferrierite in large deposits (Sand and Regis, 1966), and the high reactivity of the alkali system to produce zeolite phases at low temperatures as contrasted with the lower reactivity of alkaline-earth systems.

[1] Present Address: Mobil Research & Development Corporation, Paulsboro, New Jersey 08066

Reactor vessels used were low-carbon 304 stainless steel autoclaves of modified Morey design with 15 ml capacity. The autoclaves were sealed by annealed silver discs.

The materials used were alumina–silica gels with differing silica to alumina ratios, sodium carbonate (analytical reagent grade), sodium bicarbonate (analytical reagent grade), potassium carbonate (reagent grade), potassium bicarbonate (U.S.P.), and distilled water. The appropriate amounts of salts were mixed with gel in a mortar and pestle, and the mixture loaded into the autoclave. The required water was added, the autoclave contents were mixed, and the autoclaves were sealed as quickly as possible to prevent loss of CO_2. The sealed vessels were placed at time zero in ovens at temperature. The vessels were water-quenched immediately on termination of the run. Reproducible results were obtained with this technique.

The solid products were identified with a Philips-Norelco model 3000 X-ray diffractometer with a monochromator attachment. Exact peak locations were determined using an internal aluminum standard. A Cambridge Stereoscan Model S-4 was used to obtain the scanning electron micrographs. Sorption experiments were carried out in constant-volume constant-pressure Cahn Vacuum Electrobalance unit.

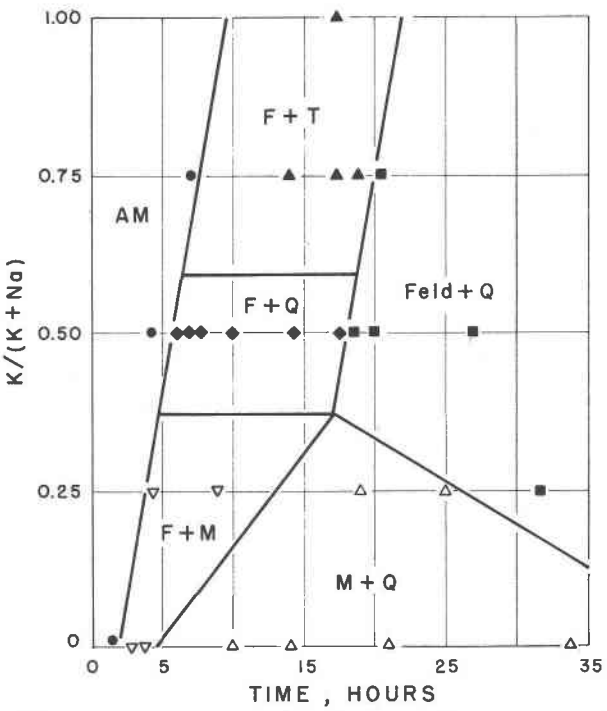

FIG. 1. Isothermal phase-transformation diagram on starting composition $3.26(Na_2O + K_2O)$–Al_2O_3–$13.5SiO_2$–$130.4H_2O$–$0.82CO_2$–$2.44(HCO_2)_2$ at 280°C. The ordinate is the K/(K + Na) ratio in the starting batch composition.
AM = amorphous, F = ferrierite, M = mordenite, Feld = feldspar, T = tridymite, Q = quartz.

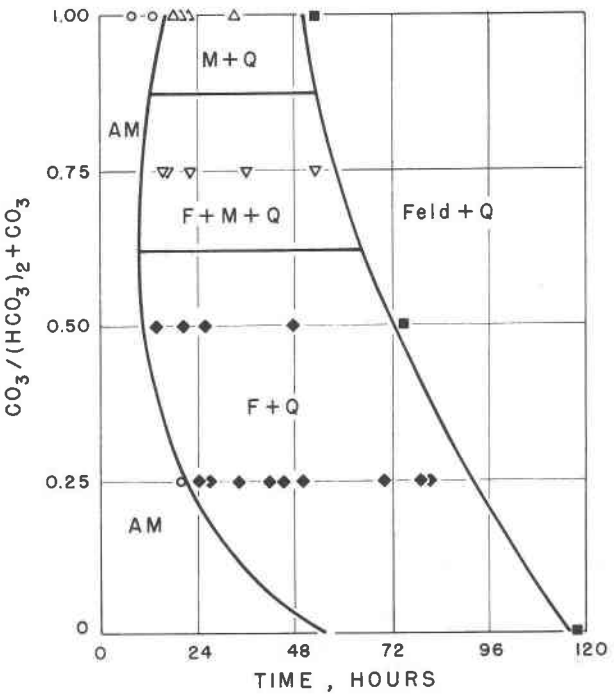

FIG. 2. Isothermal phase-transformation diagram on starting composition $1.63Na_2O$–$1.63K_2O$–Al_2O_3–$13.5SiO_2$–$130.4H_2O$–$3.26[CO_2 + (HCO_2)_2]$ at 230°C. The ordinate is the $CO_3/[(HCO_3)_2 + CO_3]$ ratio in the starting batch composition.
AM = amorphous, F = ferrierite, M = mordenite, Feld = feldspar, Q = quartz.

Results

In contrast to the pure Na_2O $(+Al_2O_3 \cdot SiO_2 \cdot H_2O)$ system, it was found that adding a combination of Na_2O–K_2O and a CO_3/HCO_3 buffer pair produced systems that yielded ferrierite reproducibly. Ferrierite was found to be metastable in such a system by observing its isothermal transformation to mordenite or feldspar as a function of time, and it was decided to study systematically the kinetics of crystallization and the phase transformation of ferrierite as a function of K/Na and CO_3/HCO_3 ratios in the reacting system. A co-precipitated alumina–silica gel with an excess of silica over that required for ferrierite was selected for use as a reactant, in order to observe the silicia phase associated with ferrierite under varying experimental conditions. Figure 1 plots the results obtained varying only the K/Na ratios at autogenous pressure at 280°C as a function of time. The

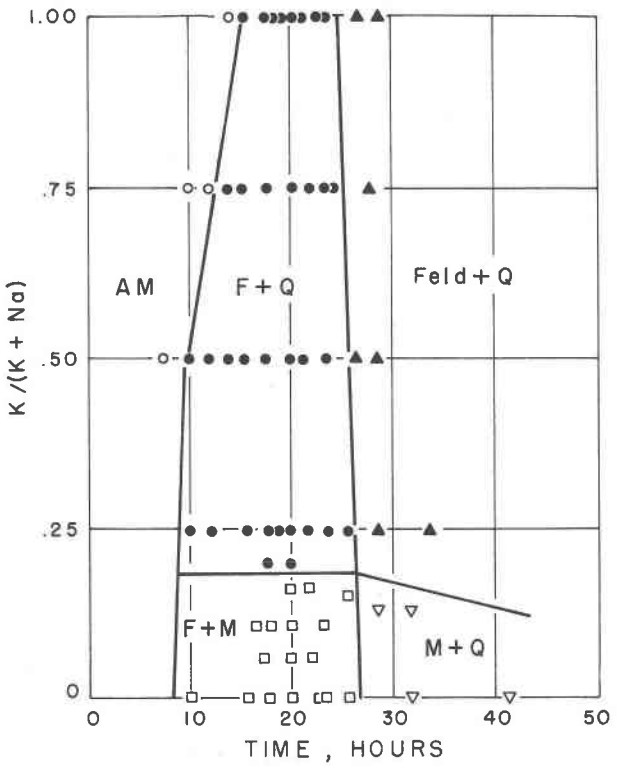

FIG. 3. Isothermal phase-transformation diagram on starting composition $3.68(Na_2O + K_2O)$–Al_2O_3–$10.38SiO_2$–$147.2H_2O$–$0.92CO_2$–$2.76(HCO_2)_2$ at 280°C. The ordinate is the K/(K + Na) ratio in the starting batch composition.
AM = amorphous, F = ferrierite, M = mordenite, Feld = feldspar, Q = quartz.

$CO_3/[CO_3 + (HCO_3)_2]$ ratio was held constant at 0.25. The metastable nature of ferrierite is evident. At high or intermediate K/(K + Na) ratios, ferrierite is associated with a silica polymorph, either quartz or tridymite. The ferrierite then transforms to feldspar and quartz. However, at batch compositions with a high Na content, mordenite was the associated phase. The ferrierite quickly transforms to mordenite and quartz which eventually transforms to the stable products, feldspar and quartz. Although it needs more study, the metastability of ferrierite might be the explanation for the coexistence of zeolite phases of very similar chemical composition, such as ferrierite and mordenite in the Fallon, Nevada, occurrence and ferrierite and clinoptilolite in the Agoura, California, occurrence. Ferrierite might have crystallized initially as a metastable phase, and was in the process of transforming to mordenite or clinoptilolite, respectively, when the systems ceased to be reactive.

Figure 2 plots the results obtained from batch compositions holding the K/(K + Na) ratio constant at 0.50 and varying the CO_3/HCO_3 ratio versus time at 230°C and autogenous pressure. The results were similar to the previous case except for the slower kinetics due to the lower temperature. When ferrierite was formed it was associated with quartz and/or mordenite. The ferrierite then was transformed to quartz and feldspar. However, ferrierite was not formed in the pure carbonate system.

Figures 3 and 4 are the phase transformation diagrams on batch compositions with a silica to alumina ratio close to that of natural ferrierites (SiO_2/Al_2O_3 = 10.0). The results plotted in Figure 3 depict the effect of the K/(Na + K) ratio on batch compositions holding the $CO_3/[CO_3 + (HCO_3)_2]$ at 0.25 at 280°C and autogenous pressure. The results obtained are similar to the results shown in Figure 1, which were obtained from a batch composition higher in silica content. However, no tridymite was formed even at higher K/(K + Na) ratios. Quartz was the only silica polymorph associated with ferrierite. At low K/(K + Na) ratios no feldspar was formed even at autoclaving times up to 200 hours. It is possible that mordenite is a stable phase in this system.

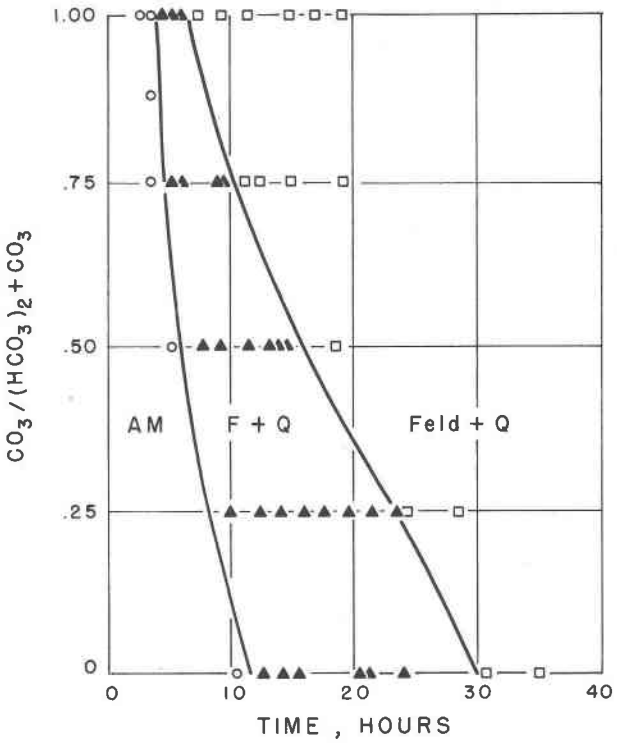

FIG. 4. Isothermal phase-transformation diagram on starting composition $1.84Na_2O$–$1.84K_2O$–Al_2O_3–$10.38SiO_2$–$147.2H_2O$–$3.68[CO_2 + (HCO_2)_2]$ at 280°C. The ordinate is the $CO_3/[(HCO_3)_2 + CO_3]$ ratio in the starting batch composition.
AM = amorphous, F = ferrierite, Feld = feldspar, Q = quartz.

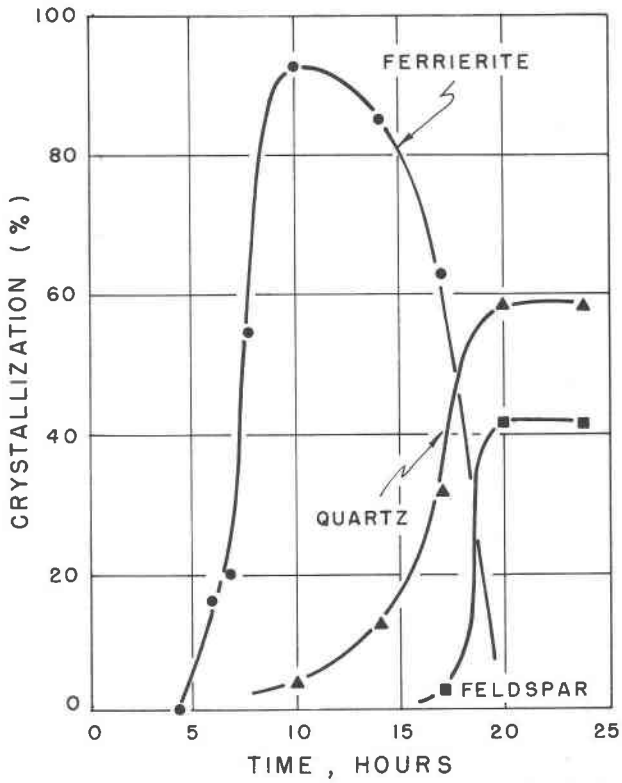

FIG. 5. Crystallization curve and transformation of ferrierite synthesized from a starting composition of $1.5Na_2O$–$1.5K_2O$–Al_2O_3–$10.47SiO_2$–$240.0H_2O$–$0.53CO_2$–$1.59(HCO_2)_2$ at 280°C.

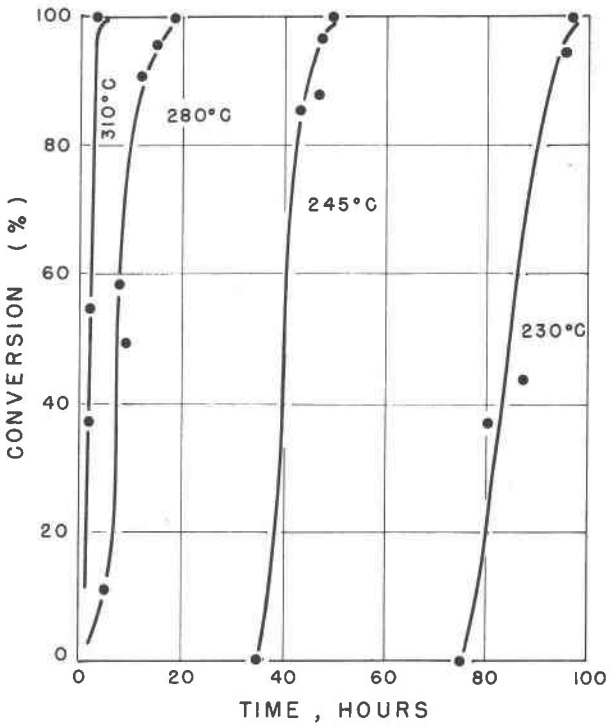

FIG. 6. Crystallization curves for ferrierite on starting composition $1.63Na_2O$–$1.63K_2O$–Al_2O_3–$13.5SiO_2$–$130.4H_2O$–$0.82CO_2$–$2.44(HCO_2)_2$.

Figure 4 gives the results obtained when the K/(K + Na) ratio was held constant at 0.50 and the CO_3/HCO_3 ratio varied at 280°C and autogenous pressure. Contrasted to Figure 2, in this system no mordenite was formed, and ferrierite is synthesized even in pure carbonate systems. The greater reactivity in carbonate systems as compared to bicarbonate systems is evidenced by the shorter nucleation times and the decrease in the size of the metastability region of ferrierite formation as the carbonate content is increased.

Figure 5 shows a quantitative representation of the ferrierite phase transformation. Crystallization of ferrierite proceeds after the induction period and follows the normal S-shaped curve. Quartz forms at the same time in small amounts as a coexisting phase. However, ferrierite is present only for a short time and transforms to feldspar and additional quartz.

Crystallization curves are given at four different temperatures for one batch composition in Figure 6. The activation energies for nucleation and crystallization can be determined from these curves. Assuming that the nucleation process is an energetically acti-

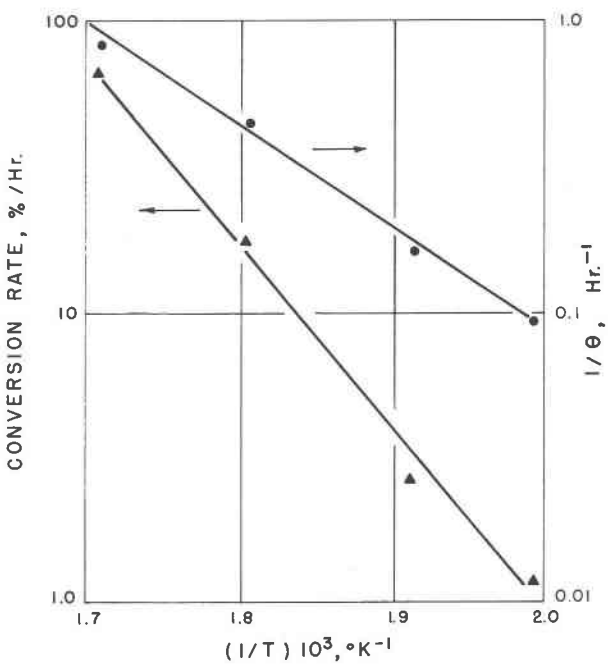

FIG. 7. Dependence of reaction rate and induction period on temperature obtained from curves in Fig. 6.

TABLE 1. Chemical analyses of samples* containing mostly (90%) synthetic ferrierite

$K_2O/(K_2O+Na_2O)$ in starting composition	0.75	0.50	0.25	0.15	0.10
$\%SiO_2$	70.90	69.50	70.60	69.10	68.43
$\%Al_2O_3$	10.83	10.50	10.73	10.40	10.35
$\%K_2O$	10.10	9.25	7.26	4.80	4.22
$\%Na_2O$	0.24	0.52	2.10	3.68	4.85
$\%H_2O$	6.18	8.24	8.31	13.55	14.05

Synthesized from starting compositions $3.84(Na_2O+K_2O)$-Al_2O_3-$10.38SiO_2$-$147.2H_2O$-$0.92CO_2$-$2.76(HCO_2)_2$ at 280°C and autogenous pressure.

TABLE 3. Calculated unit-cell compositions of ferrierites obtained as a function of K/(K + Na) ratios in the starting composition

K/(K+Na)	
.75	$K_{6.06}Na_{.21}Al_6Si_{30}O_{72} \cdot 9.7H_2O + 3.3\ SiO_2$ Excess 0.27
.50	$K_{5.73}Na_{.48}Al_6Si_{30}O_{72} \cdot 13.3H_2O + 3.7\ SiO_2$ Excess 0.21
.25	$K_{4.41}Na_{1.92}Al_6Si_{30}O_{72} \cdot 13.1H_2O + 3.5\ SiO_2$ Excess 0.33
.15	$K_{3.00}Na_{3.51}Al_6Si_{30}O_{72} \cdot 22.1H_2O + 3.9\ SiO_2$ Excess 0.51
.10	$K_{2.64}Na_{4.62}Al_6Si_{30}O_{72} \cdot 23.1H_2O + 3.7\ SiO_2$

vated process and is the limiting step in the induction period, the activation energy for nucleation, E_n, can be determined by the relation:

$$\frac{d \ln (1/\theta)}{d (1/T)} = \frac{E_n}{R}$$

where θ is the induction period (Hsu, 1971).

A similar analysis can be made to determine the activation energy for crystallization E_c, from the Arrhenius equation.

Figure 7 shows the dependence of conversion rate and induction period on temperature for ferrierite crystallization. The apparent activation energies for nucleation and crystallization calculated from this plot are 9.7 kcal/g mole and 16.7 kcal/g mole, respectively.

Chemical analyses for selected ferrierite and feldspar samples are given in Tables 1 and 2, respectively. Table 3 lists calculated unit-cell compositions as a function of K/(K + Na) ratios in the starting composition. The excess silica is the amount of the silica polymorph formed in the syntheses. A definite preference for potassium is seen in the structure of ferrierite. A partitioning function such that ferrierite incorporates nearly all the potassium available in predominantly sodium systems is evident. The preference for potassium is such that 92 percent of the cations in ferrierite are potassium when the batch composition contains equal amounts of sodium and potassium. This partitioning function is shown in Figure 8. The calculated excess silica remains constant. The water content increases with the more hydrated sodium cation.

The analyses of the feldspars formed by the transformation of ferrierite show that the preference for potassium continues. Formation of K-feldspar in natural occurrences from zeolite precursors in tuffs that were never deeply buried has been documented in recent studies and reviewed by Sheppard and Gude (1973). Sheppard and Gude (1973) have also shown that zeolites either transform to analcime and then to K-feldspar or directly to K-feldspar. Such an origin for K-feldspar is further substantiated by the work of Nemecz and Varju (1962) who synthesized K-feldspar by heating clinoptilolite with a solution of KOH at 250°C for 12 hours.

Synthetic K-ferrierite was treated with a 1.0N HCl solution three times at 70°C. Chemical analyses of this ion-exchanged ferrierite revealed that not all the potassium was exchanged. On the basis of an idealized unit cell containing 6.0 monovalent cations, 1.67 K^+ ions were not removed. These cations are probably situated in the large cavities which connect the

TABLE 2. Bulk chemical analyses of products of the transformation of ferrierite to primarily feldspar with quartz

K/(K+Na)starting composition	1.00	0.75	0.50	0.25
$\%SiO_2$	71.16	71.60	69.70	70.55
$\%Al_2O_3$	12.95	13.50	11.66	12.01
$\%K_2O$	13.45	11.15	13.20	13.60
$\%Na_2O$	-----	0.68	1.71	0.20
$\%H_2O$	2.06	3.07	4.52	3.75

Synthesized from starting compositions $3.26(Na_2O+K_2O)$-Al_2O_3-$13.5SiO_2$-$230.4H_2O$-$0.8CO_2$-$2.44(HCO_2)_2$ at 280°C and autogenous pressure.

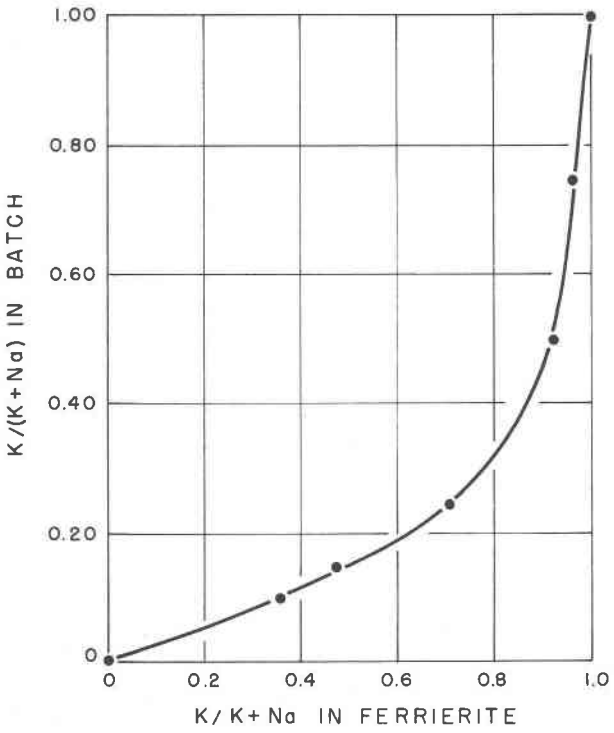

FIG. 8. Partitioning function showing dependence of K/(K + Na) ratio in ferrierite on the K/(K + Na) ratio in the starting composition.

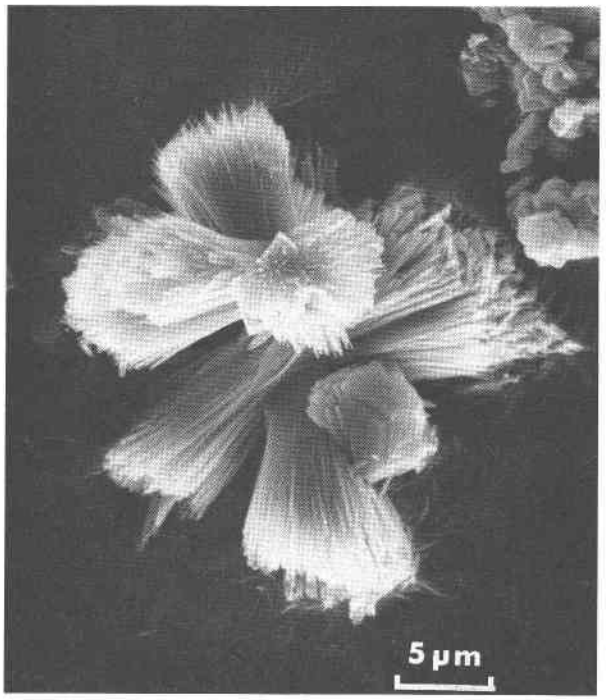

FIG. 10. Platy and spindle-fiber type ferrierite crystals. X-ray microprobe analysis reveals that both types are essentially pure K-ferrierite. The crystals in the upper right are pure silica-quartz crystals with ferrierite in this metastability region. Starting composition: $1.63NaO$–$1.63K_2O$–Al_2O_3–$13.5SiO_2$–$130.4H_2O$–$0.88CO_2$–$2.44(HCO_2)_2$, 230°C, 92 hours.

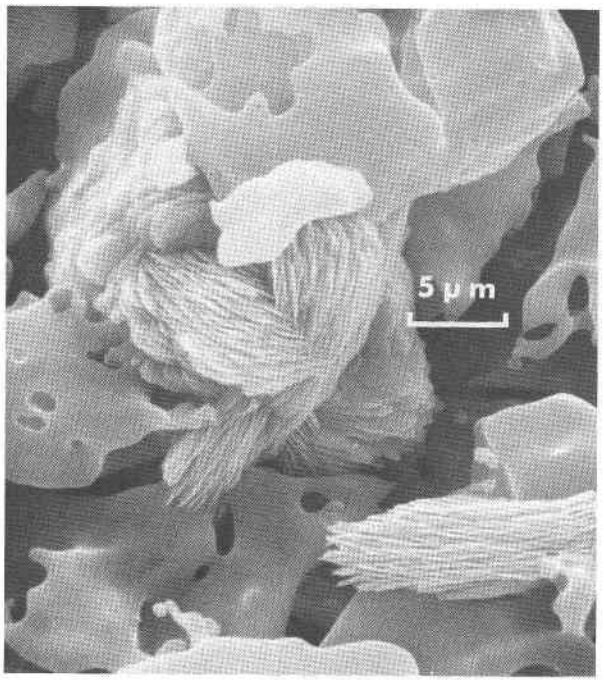

FIG. 9. Platy ferrierite crystals growing in an untransformed gel matrix. Starting composition: $1.63Na_2O$–$1.63K_2O$–Al_2O_3–$13.5SiO_2$–$130.4H_2O$–$0.82CO_2$–$2.44(HCO_2)_2$, 230°C, 40 hours.

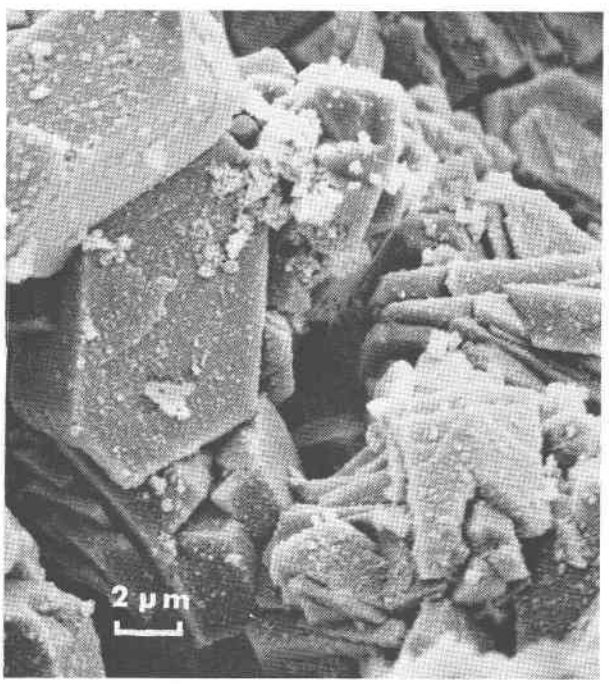

FIG. 11. K-feldspar crystals formed by the transformation of ferrierite. Starting composition: $0.82NaO$–$2.44K_2O$–Al_2O_3–$11.1SiO_2$–$130H_2O$–$0.82CO_2$–$2.44(HCO_2)_2$, 280°C, 18 hours.

minor channel system to the main channel system. There are two of these cavities per unit cell and they have a diameter of 7.0Å. The cavities are connected to the main channel system by windows 4.7Å by 3.4Å. An anhydrous K^+ ion with a diameter of 2.66Å should have no difficulty passing through this window and being exchanged. However, a hydrated K^+ ion with a diameter of 3.80Å would be trapped within the cavity, as is hydrated Mg^{2+} in the Kamloops variety of ferrierite (Vaughan, 1966).

X-ray powder diffraction data are similar to those published by Staples (1955) for the Kamloops Lake, British Columbia occurrence. Detailed comparative X-ray powder diffraction data for synthetic K–ferrierite are given by Cormier (1974).

The unit-cell constants are for a ferrierite synthesized from batch composition $1.63Na_2O$–$1.63K_2O$–Al_2O_3–$13.5SiO_2$–$260.8H_2O$–$2.44(HCO_2)_2$–$0.82CO_2$ at 280°C for 18 hours under autogeneous pressure. They were calculated using a three-cycle, least-squares refinement and are a = 19.11(5), b = 14.10(3), c = 7.48(2) Å.

Adsorption experiments on Na- and K–ferrierite indicate that the ferrierite pore system is partially blocked. At 25°C ferrierite did not absorb isohexane, isobutane, or benzene. The largest molecule adsorbed was propane (critical diameter 4.89Å), and propane was adsorbed very slowly and in limited amounts (1.5 wt. %).

Scanning electron micrographs are shown in Figures 9–11.

Conculsions

The results of the isothermal phase-transformation diagrams are informative in interpreting the origin of the ferrierite occurrences. Although not conclusive, it appears from the experimental data that ferrierite forms at temperatures well above diagenetic conditions. Ferrierite was not formed at temperatures below 210°C in this study, and at 210°C ferrierite was a minor phase associated with mordenite. On the basis of present information, an estimated temperature for natural ferrierite formation seems to be 200–400°C. The experimental data showing ferrierite–mordenite–tridymite–quartz phase relationships most closely resemble the Pershing County, Nevada, ferrierite occurrence in altered bedded pyroclastics. The metastability of ferrierite, as witnessed by the isothermal phase-transformation diagrams, might be the explanation for the occurrence of another zeolite with similar chemical composition, such as mordenite with ferrierite in the Nevada occurrence and clinoptilolite with ferrierite in the Agoura, California, occurrence. Instead of being coexisting phases as regarded in the usual equilibrium context, ferrierite might have crystallized initially as a metastable phase and transformed partly to the other phases before reaction stopped. The occurrence of the silica polymorphs, quartz and tridymite, in ferrierite deposits can also be explained from the isothermal phase-transformation diagram in Figure 1.

From the chemical composition data, it can be seen that ferrierite preferentially incorporated potassium over sodium into its structure. In fact, in batch compositions with low potassium content essentially all the available potassium is incorporated in the structure. H exchange experiments suggest that all the potassium cannot be ion-exchanged, indicating the presence of hydrated potassium ions in the two cavities per unit cell.

The transformation of ferrierite to K–feldspar is useful in explaining the transformation of zeolites either to analcime and then to K–feldspar or directly to K–feldspar in natural occurrences as reported by Sheppard and Gude (1973).

These synthetic ferrierites, as with naturally occurring ferrierites, do not exhibit the adsorption properties expected of an intermediate port-size zeolite. The presence of a ten-membered ring would indicate the capability of selectively sorbing molecules of a critical size of from 5.5–6.0Å while excluding molecules of larger molecular dimensions. The largest molecule adsorbed by ferrierite was propane with a critical diameter of 4.89Å. This indicates that the main channels in the ferrierite structure are partially blocked. Possible explanations of this could be the presence of structural faults, amorphous starting material caught within the pore system, or the position or nature of the cations.

Acknowledgments

Financial assistance provided by a teaching assistantship from Worcester Polytechnic Institute and from grants given by Union Oil Corporation and Mobil Oil Corporation is gratefully acknowledged.

Appreciation is expressed to Jeol Inc., Medford, Massachusetts, for scanning electron micrographs, to Norton Company for chemical analyses, and to Mr. Peter Hatgelakas for laboratory assistance.

References

Alietti, A., E. Passaglia and G. Sciani (1967) A new occurrence of ferrierite. *Am. Mineral.* **52**, 1562–1563.

Barrer, R. M. and D. J. Marshall (1965) Synthetic zeolites related to ferrierite and yugawaralite. *Am. Mineral.* **50**, 484–489.

CORMIER, W. E. (1974) *Synthesis and Properties of Na–, K–, and Na,K–Ferrierites.* M.S. Thesis, Worcester Polytechnic Institute, Worcester, Massachusetts.

GRAHAM, R. P. D. (1918) On ferrierite, a new zeolitic mineral from British Columbia; with notes on some other Canadian minerals. *Trans. Roy. Soc. Canada* [3], **12,** Sect. IV, 185–201.

HAWKINS, D. B. (1967) Zeolite studies I. Synthesis of some alkaline earth zeolites. *Mater. Res. Bull.* **2,** 951–958.

HSU, A. C. T. (1971) Nucleation and crystal proliferation kinetics, amorphous-crystalline transformation of basic copper carbonates. *Am. Inst. Chem. Eng. J.* **17,** 1311–1315.

KERR, I. S. (1966) Structure of ferrierite. *Nature,* **210,** 294–295.

NEMECZ, E. AND G. VARJU (1962) Sodium bentonitization, clinoptilolitization adultarization in the rhyolitic tuffs of the Szerencs piedmont area. *Acta Geologica,* **6,** 389–427.

SAND, L. B. (1968) Synthesis of large-port and small-port mordenites. In, *Molecular Sieves.* Soc. Chem. Ind. Special Publ., London, 71–77.

——— AND A. J. REGIS (1966) Occurrence of ferrierite, Pershing Co., Nevada. [Abstr.] *Geol. Soc. Am. Annual Mtgs. Program,* 189.

SENDEROV, E. E. (1963) Crystallization of mordenite under hydrothermal conditions. *Geokhimiya,* **9,** 820–829.

SHEPPARD, R. A. AND A. J. GUDE (1973) Boron-bearing potassium feldspar of authigenic origin in closed basin deposits. *J. Res. U.S. Geol. Surv.* **1,** 377–382.

STAPLES, L. W. (1955) X-ray investigation of ferrierite, a zeolite. *Am. Mineral.* **40,** 1095–1099.

VAUGHAN, P. A. (1966) The crystal structure of the zeolite ferrierite. *Acta Crystallogr.* **21,** 983–990.

WISE, W. S., W. J. NOKLENERG AND M. KOKINOS (1969) Clinoptilolite and ferrierite from Agoura, California, *Am. Mineral.* **54,** 887–895.

Manuscript received, December 17, 1975; accepted for publication, July 14, 1976.